ELSEVIER

Current Opinion in Colloid & Interface Science 6 (2001) 223–235

Current Opinion in Colloid & Interface Science

www.elsevier.nl/locate/cocis

The interaction of two fluid phases in fractured media

Robert J. Glass[a,*], Harihar Rajaram[b], Michael J. Nicholl[c], Russell L. Detwiler[b]

[a] *Flow Visualization and Processes Laboratory, Sandia National Laboratories, Albuquerque, NM 87185-0735, USA*
[b] *Department of Civil, Environmental, and Architectural Engineering, University of Colorado, Boulder, CO 80309-0428, USA*
[c] *Department of Materials, Metallurgical, Mining and Geological Engineering, University of Idaho, Moscow, ID 83844-3024, USA*

Abstract

In fractured porous media, interactions between immiscible fluid phases within the fractures place a critical control on system behavior. A key component of the interactions is the geometry, or structure, of the respective phases. Over the past 10 years, process-based experiments have greatly increased our understanding of phase structure development within individual fractures. In the past 2 years, new calculational models that incorporate some of this understanding have further demonstrated the influence of phase structure on flow and transport within the phases, and inter-phase mass transport. These computational models can now be applied to consider the efficacy and parameterization of constitutive relations for a subset of two-phase situations. Full understanding of the morphology, connectivity, and temporal dynamics of phase structure in rough-walled fractures is yet to be developed, and is a promising area for further research.

Keywords: Fractures; Two-phase flow; Transport; Phase dissolution; Percolation

1. Introduction

Flow and transport in fractured porous media are challenging problems, primarily because two systems with extremely different hydraulic properties (fractures, porous media) coexist and interact. Flow and transport occur, both within each system, and between the two. This first level of complexity is further exacerbated when more than one fluid phase is present; then, capillarity, accessibility, and gravity compete with viscous forces to control hydraulic properties of the system. For example, capillarity alone can reverse single-phase behavior; i.e. a flow conduit may be transformed into a flow barrier for one of the phases. For multi-phase, immiscible fluid flow conditions, phase structure within individual fractures and the fracture network (i.e. the geometry that is filled by each phase) ultimately controls the fluid pressure-saturation relations, permeability to each phase, solute dispersion within each phase, and inter-phase mass transfer; in addition, fracture phase structure also controls flow and transport through the surrounding porous matrix blocks by affecting their hydraulic contact [1••,2••].

Considering the complexity of flow and transport in fractured porous media, and that phase structure within individual fractures places a critical control on system response, we focus in this paper on the rich variety of behavior that occurs within a single fracture at the sub-m scale under conditions where two phases interact. We constrain our discussion to neglect exchange with the adjacent matrix, reactive transport, more than two phases, film flow, and phase transitions; we also consider only incompressible flow in the absence of thermal and mechanical effects. We begin with capillary-dominated phase displacement, and then add the influence of viscous and gravity forces. Next, we consider flow and transport within a phase, and conclude with inter-phase mass transfer. Because the study of two-phase flow in fractures is embryonic, we explain the state of understanding in each of these

* Corresponding author. Tel.: +1-505-844-5606.
E-mail address: rjglass@sandia.gov (R.J. Glass).

1359-0294/01/$ - see front matter
PII: S1359-0294(01)00086-3

topics, and use recently developed modeling capabilities to illustrate the important control of phase structure throughout.

2. Phase displacement processes: capillary-dominated

Under quasi-static flow conditions, phase structure in a horizontal fracture will be controlled by capillary forces; in general, the non-wetting phase will be found in large apertures and the wetting phase in small ones. The Laplace–Young equation relates surface tension (T) and interfacial curvature to the pressure jump across the curved interface (ΔP):

$$\Delta P = T\left(\frac{1}{r_1} + \frac{1}{r_2}\right) \tag{1}$$

where r_1 and r_2 are the two principle radii of curvature. The first principal radius of curvature (r_1) is taken normal to the plane of the fracture, and is given by $r_1 = b/2\cos\alpha$, where b is the local aperture, and α is the fluid–fluid–solid contact angle. Curvature in the plane of the fracture (r_2) is considered not to contact the fracture surface, and therefore is not constrained by a contact angle. If it is assumed that interfacial curvature in the plane of the fracture is negligible ($r_2 \to \infty$), and that lack of access does not limit the distribution of phases, then phase structure-pressure relationships will conform to a two-dimensional standard percolation (SP) process. A variety of interesting results comes from application of SP theory to a random aperture field; the most important are that the phase structure is fractal, and that a critical pressure exists where one phase forms an infinite connected cluster isolating the other phase [3,4•].

Experimental investigations of quasi-static phase displacement in horizontal fractures have shown irreversible and hysteretic behavior [5,6•], and thus question the validity of SP methods for predicting phase structure. The assumption of reversible equilibrium inherent in SP requires all apertures to be in a state of mutual and instantaneous communication. Three main communication processes may exist; flow through the matrix that connects all apertures, film flow along the fracture walls, and diffusional processes. To satisfy equilibrium, phase displacement must occur slowly with respect to the fastest communication process. For a large number of situations, either communication processes do not exist, or, relative to them, phase displacement occurs rapidly. In such situations, accessibility places an additional control on phase structure. In order for an aperture to be accessible to a given phase, it must be adjacent to an aperture that is not only occupied by that phase, but is also connected to a source (or sink). Placing this condition on both phases leads to entrapment; i.e. apertures disconnected from a sink cannot escape and may not be replaced by the other phase. To include phase accessibility, an invasion percolation (IP) process, as introduced by Wilkinson and Willemsen [7] can be used in combination with Eq. (1), once again neglecting in-plane interfacial curvature ($r_2 \to \infty$). However, experimental evidence also shows IP to be deficient, as quasi-static displacements in horizontal analog fractures often exhibit macroscopic fronts, decreased phase entrapment on invasion, and compact entrapped-phase dissolution [8,9•,10•].

Recent work has shown that deficiencies in IP may be overcome by specifically including the influence of in-plane curvature (r_2) in the calculation of invasion pressure [8,11••]. Modification of the IP process to include the dynamic calculation of in-plane curvature (MIP) at the evolving interface produces phase structures that closely resemble experimental observations, for both wetting and non-wetting displacements. The importance of in-plane curvature was considered systematically by Glass et al. [11••]; they defined a simplified pressure equation, in which a dimensionless curvature number (C) weighs the relative strength of the two curvatures (r_1,r_2). Simulations show that as C increases from 0 (the IP limit), the phase displacement structure transitions from highly complicated to macroscopically smooth. To illustrate this influence, Fig. 1 shows displacement simulations on a spatially correlated random aperture field with a factor of two difference in C. The full sensitivity study shows that fracture phase saturations, the number of entrapped phase clusters, and the maximum entrapped cluster size are not only highly dependent on C, but exhibit a differential response to C between wetting and non-wetting invasion that is independent of contact angle hysteresis. Therefore, macroscopic effective properties or models dependent on underlying phase structure (e.g. pressure-saturation relations, relative permeability, solute dispersion, inter-phase mass transfer, fracture-matrix interaction) will exhibit strong functional dependency on C that is different for wetting and non-wetting invasion.

3. Phase displacement processes: addition of gravity and viscous forces

Inclusion of gravity and viscous forces into the displacement process can act to either destabilize the front (i.e. initiate gravity or viscous fingering), or decrease capillary-controlled complication (i.e. further stabilize) to produce a flattened front with less phase entrapment behind. In the absence of capillary forces, linear stability analysis suggests that displace-

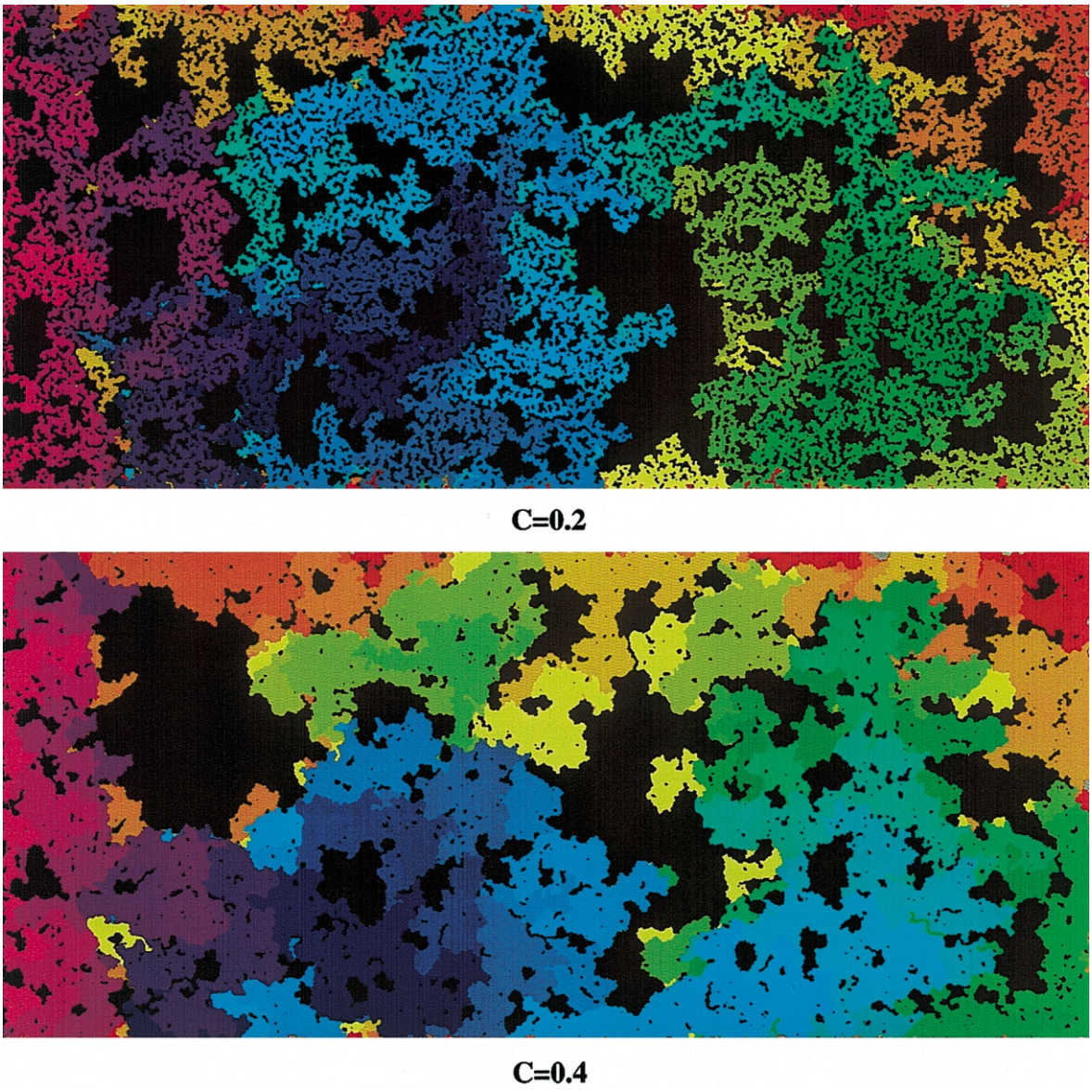

Fig. 1. Phase displacement with only capillary forces: influence of curvature number, C. An MIP model including both aperture induced and in-plane curvature is used to simulate wetting phase invasion from the left in a spatially correlated random aperture field ($\sigma/\langle b \rangle$ of 0.24 and size of ~160 by ~350 spatial correlation lengths) measured by Detwiler et al. [38••]. Long and right sides of the fracture are open for defending non-wetting phase to escape. Black denotes entrapped non-wetting phase, while the color sequence purple–blue–green–yellow–orange–red denotes invasion order. The top invasion structure is for $C = 0.2$, while the bottom is for $C = 0.4$ and show final wetting phase saturations of 0.47 and 0.77, respectively. The factor of two increase in C can be interpreted as a corresponding increase in mean aperture or contact angle, or decrease in the variance or correlation length of the random field [11••].

ment of one incompressible fluid (subscript $_2$) by another (subscript $_1$) in a smooth-walled fracture (Hele–Shaw cell) will be subject to gravity or viscous instability when:

$$\frac{U}{k}(\mu_1 - \mu_2) + g\cos\theta(\rho_1 - \rho_2) > 0 \qquad (2)$$

where μ is the fluid dynamic viscosity, ρ the fluid density, U the interfacial velocity, g the gravitational acceleration, k the intrinsic permeability, and θ the included angle between vertically downwards and the direction of displacement along the fracture plane. While very simplistic, this analysis contains the rudiments of both the destabilizing and stabilizing influences. Most research in the fluid mechanics literature has concentrated on viscous-driven fingering in smooth-walled Hele–Shaw cells in the absence of gravity (e.g. [12]). To our knowledge, studies of viscous fingering in variable-aperture fractures have yet to be accomplished.

Gravity-driven fingering has been studied in rough-walled analog fractures for air/water systems by Nicholl et al. [13–16••]. In initially dry fractures, experiments and dimensional analysis show that the

velocity of fingers formed under steady supply conditions display a functional relationship with volumetric flow rate, gravitational gradient, and finger width. In turn, finger width is controlled by finite amplitude perturbations present at initiation (which is influenced by flow rate and gravitational gradient). Fingers formed in an initially dry aperture field provide preferential pathways for subsequent fingers [13,15]. In contrast to observations in porous media, where uniform initial moisture has been shown to stabilize displacement of the wetting phase (e.g. [17]), initial moisture does not necessarily stabilize fracture flow where the initial moisture structure is poorly connected [15]; however, enhanced connection associated with micro roughness or a wet matrix may provide a stabilizing influence.

Flow pulsation and/or blob flow in fractures were noted in both early, gravity-driven fingering studies [13–16••] and during the simultaneous flow of two fluids in horizontal fractures [18,19•]. In both of these situations, local interactions of the wetting and non-wetting fluids yield potentially chaotic system dynamics [2••]. Several more recent studies have further underscored the importance of both gravity and viscous forces to create complicated dynamics [20•] and mobilize entrapped phase [21]. In all of these studies, it is assumed that fingertip length, flow pulsation, or mobilization are dependent on simple ratios of capillary, gravity, and viscous forces. However, Zhong et al. [22•] have recently shown the mobilization of entrapped phase in a horizontal fracture to be 'path' dependent. They found that when the importance of capillary relative to viscous forces is reduced, either by increasing viscous forces (flow rates), or by decreasing capillary forces with a miscible displacement (lowering of interfacial surface tension with a surfactant flood), differences in active micro-scale mobilization processes lead to different final entrapped-phase saturations and structures for the same capillary/viscous ratio.

Calculational models for phase displacement that honor the rich behavior occurring under the competing influences of capillary, viscous, and gravitational forces are in their infancy. While solution of the Navier–Stokes equations with the relevant inter-phase boundary conditions (including dynamic contact angles) at present seems intractable at the scale of individual fractures, approaches based on further modifications of MIP show great promise. MIP with in-plane curvature can be extended to include phase density differences and reproduce both gravity stabilized and destabilized displacements through fractures [8]. As illustrated in Fig. 2 top, simulations show the stabilizing influence of gravity to decrease complication of the displacement front, with a corresponding decrease in entrapped phase saturation, complication, and cluster size [Glass, unpublished]. For gravity-destabilized displacements, where the phase structure has been found to fragment behind the fingertip [14], criteria for the re-invasion of apertures by the displaced phase must include a gravity siphon within the finger. An illustrative simulation employing such an approach is shown in Fig. 2 bottom and matches experimental data well [Glass, unpublished]. In-plane curvature is found to damp the fragmentation process, yielding a macroscopic fingertip, with representative phase structure and blob flow behind. This is in contrast to a simpler conceptualization of the re-invasion process that neglects in-plane curvature and leads to fragmentation at the aperture correlation scale, even in horizontal fractures [23].

Viscous forces can also be incorporated into forms of MIP, with applications to date only for porous media [24•,25,26]. In the simplest approach, viscous stabilized displacements include a linear gradient similar to that for phase density differences. For this case, the simulation shown in Fig. 2 top also illustrates a similarly stabilized viscous displacement. Viscous destabilized displacements have not yet been considered using an MIP approach; however, in porous media and Hele–Shaw cells, diffusion-limited aggregation (DLA) has been used (e.g. [4•]). The DLA process produces highly complicated structures dominated by noise; however, manipulating the conditions for local growth can produce more compact structures that provide a first-order approximation of surface tension (e.g. [27]).

4. Flow processes within a phase

At low Reynolds number, the Stokes equations are expected to fully describe steady flow of a homogeneous, incompressible fluid phase in a variable aperture fracture. To circumvent the data and computational requirements for numerical solution of the three-dimensional Stokes equations, a two-dimensional, depth-averaged approximation known as the Reynolds equation is commonly used to simulate fracture flow. Although attractive from a computational standpoint, this approach assumes that local flow exhibits a parabolic velocity profile, as would occur between parallel plates. Analytical studies (e.g. [28•,29]) suggest that the Reynolds equation will be appropriate for fracture flow at small Reynolds number, provided that aperture mean and variance are significantly smaller than the characteristic length scale of the aperture variation (i.e. spatial correlation).

Simulation of Stokes flow in two-dimensional fracture cross-sections using continuum methods [30], and more recently, lattice–Boltzmann or lattice–gas methods [31•,32,33], suggest that the assumption of a

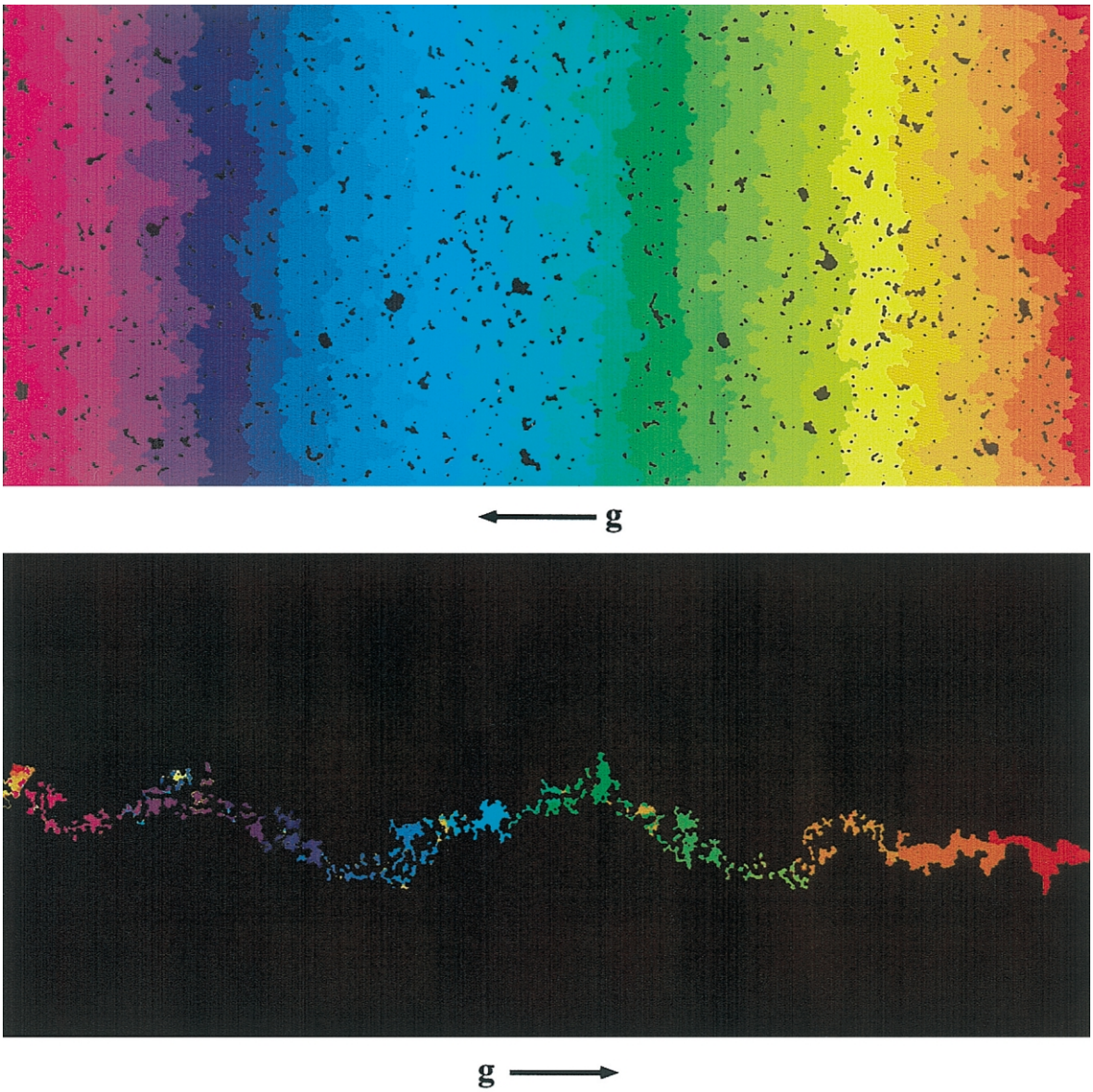

Fig. 2. Phase displacement with the addition of gravity forces: stabilizing vs. destabilizing. An MIP model including both aperture-induced and in-plane curvature, as well as gravity forces, is used to simulate wetting phase invasion from the left in the same spatially correlated random aperture field as used in Fig. 1 with $C = 0.4$. In the top simulation, gravity is acting to the left (stabilizing); black denotes entrapped non-wetting phase, while the color sequence purple–blue–green–yellow–orange–red denotes invasion order. In the bottom simulation, gravity is acting to the right (destabilizing); color once again denotes invasion order at the point where the finger has reached the bottom of the aperture field with black denoting nonwetting phase. For the gravity-destabilized case, MIP has been augmented to include criteria for the re-invasion of apertures with the non-wetting phase. Note the saturated fingertip at the bottom of the figure, with the fragmented wetting phase trail behind. Intermixed color out of sequence shows locations where phase structure has changed as pulses of invading phase coursed downward to supply the growing tip.

parabolic velocity profile may not be universally valid; deviation from a parabolic profile has also been observed experimentally [34]. Three-dimensional simulation of Stokes flow in a range of synthetic aperture fields has demonstrated that the Reynolds equation may overestimate flow by as much as a factor of two [35•]. Experiments in replicas of natural fractures (e.g. [36,37]) have produced conflicting results regarding applicability of the Reynolds equation; direct evaluations are hindered by the difficulty in obtaining aperture data at appropriate accuracy [38••]. A study that obtained such data has recently been accomplished by Nicholl et al. [39•], who considered two analog fractures specifically designed to test the Reynolds equation. Simulations on highly accurate aperture data overestimated experimental flow rates by 22–47%. They concluded that head loss associated with three-dimensional flow components

was the root cause of the discrepancy, and that local corrections to the Reynolds equation modified, but did not eliminate, the discrepancies.

At the macroscopic scale, effective medium theory has been employed to estimate a hydraulic aperture (b_h), which, when used in the cubic law, would adequately represent fracture transmissivity. Gelhar [40] showed that for lognormal aperture distributions, b_h is the geometric mean of the distribution; Zimmerman and Bodvarsson [28•] discuss other estimates for b_h. For two-phase conditions, it is common to express the effective permeability to a given phase (k_f) relative to permeability under single-phase conditions (k_s); fracture relative permeability (k_r) is then given by: $k_r = k_f/k_s$. Early efforts to calculate k_r used either SP [41] or IP [42] to define phase structure as a function of pressure, and then computed flow within each phase using the Reynolds equation. While limited due to the use of SP and IP algorithms for phase structure, results of these initial studies suggested the importance of phase interference in determining k_r. Subsequent experiments within a horizontal fracture with concurrent two-phase flow further emphasized the importance of phase interference, with k_r for wetting and non-wetting phases summing to much less than [19•].

In the absence of gravity or viscous fingering, the displacement of one phase by another in fractures much larger than the aperture correlation scale leads to a 'satiated' state, where the defending phase becomes fully entrapped. For these conditions, experiments by Nicholl and Glass [9•], where the entrapped phase structure was varied within a measured aperture field, suggest that k_f differs from k_s due to a change in the statistics of the flowing apertures, reduced cross-sectional area available for flow, and in-plane tortuosity induced by the entrapped phase. They also noted that there was little difference in k_r between trials at similar wetting phase saturation, even though the phase structures (and transport behavior) were vastly different. Combination of these observations with effective medium theory yields a conceptual model [43•] for satiated relative permeability (k_{rs}):

$$k_{rs} = \tau S_f \underbrace{\left[\frac{\langle b_f\rangle^2}{\langle b\rangle^2}\right]}_{A} \underbrace{\left[\left(1+\frac{9\sigma^2}{\langle b\rangle^2}\right)^{1/2}\left(1+\frac{9\sigma_f^2}{\langle b_f\rangle^2}\right)^{-1/2}\right]}_{B} \quad (3)$$

where τ represents in-plane tortuosity, S_f saturation by the flowing phase, $\langle b\rangle$ mean aperture, and σ^2 aperture variance; subscripted parameters are taken only over apertures filled by the flowing phase, as opposed to all apertures (no subscript). Of these factors, τ was found to be the most important, followed by S_f, (A), and finally, (B).

To further illustrate the importance of phase structure on flow within the fracture, Fig. 3 shows streamlines from examples of flow simulations within the final satiated phase structures shown previously in Fig. 1. Where the fracture is filled primarily by the flowing phase, streamlines are nearly linear and exhibit short wavelength fluctuations caused by local aperture variability. However, on a macroscopic scale, the entrapped phase introduces significant tortuosity by obstructing flow, and this tortuosity greatly decreases the permeability between the two fields. As presented in Sections 2 and 3, if we consider that beyond C, the angle of the fracture with respect to gravity, fluid densities and viscosities, invasion direction (gravity/viscous stabilized/destabilized), displacement velocity, as well as initial and boundary conditions, all influence phase structure, we see that the parameterization of an effective property such as relative permeability may be quite complicated.

5. Transport processes within a phase

Within a flowing phase, dispersion of a conservative solute results from interaction between diffusion and advection. The Peclet number ($Pe = V\langle b\rangle/D_m$, where D_m is the molecular diffusion and V the mean flow velocity) weighs the relative importance of each. Additionally, velocity will vary, both across the fracture aperture (approximately parabolic velocity profile) and in the plane of the fracture (heterogeneity in the aperture field and the morphology of any entrapped phase). To understand the interaction between diffusion and advection in a highly variable velocity field, it is useful to consider parametric models that describe the influence of velocity variations on the effective longitudinal dispersion (D_L) as a function of aperture field statistics, mean velocity through the fracture, and phase saturation/structure.

For steady, single-phase flow between parallel plates, D_L results solely from the parabolic velocity profile across the aperture (i.e. Taylor dispersion) and is proportional to Pe^2. In a variable aperture field, in-plane velocity variations give rise to geometric dispersion or 'macrodispersion', with D_L proportional to Pe. Gelhar [40] used stochastic analysis, based on the depth-averaged velocities predicted by the Reynolds equation, to derive a theoretical expression for D_L in stationary random-aperture fields proportional to the variance and the correlation length of the log-aperture field, and the mean velocity (or equivalently, Pe) in the fracture. Laboratory-scale solute transport experiments in saturated (single-phase) variable-aperture fractures have exhibited a non-linear relationship

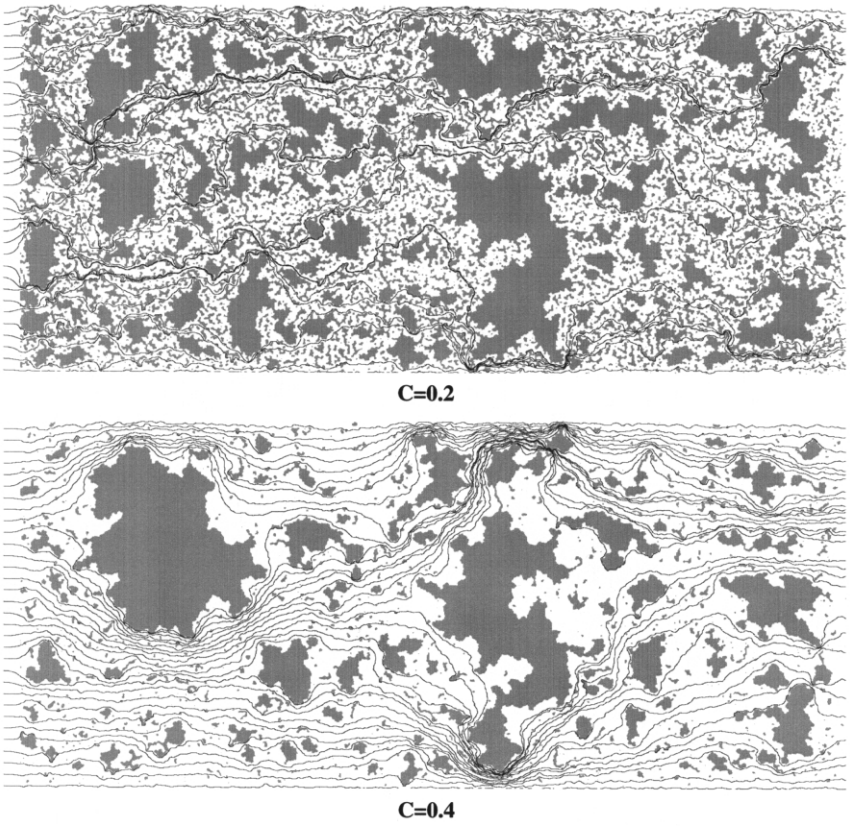

Fig. 3. Flow within fractures containing an entrapped phase: influence of curvature number, C. Using the approach of Nicholl et al. [43•], the Reynolds equation is solved within the wetting phase for flow from left to right in the fracture with final satiated phase structures of Fig. 1. The flowing wetting phase is shown in white, gray denotes entrapped non-wetting phase, and streamlines are in black. Constant head boundary conditions were established in large aperture 'manifolds' added to each end of the phase structure; the long edges were held as no-flow boundaries. Streamlines begin uniformly spaced within the inflow manifold, converge to enter the phase structure, and then proceed to the downstream end of the fracture (right side). Macroscopic tortuosity induced by the entrapped phase and satiated relative permeabilities (0.056 for $C = 0.2$ and 0.177 for $C = 0.4$) are representative of experimental observations [9•,10•,43•].

between D_L and Pe [44,45•], suggesting that D_L may result from a combination of Taylor dispersion and macrodispersion. Based on a scaling analysis, Roux et al. [46•] suggested that D_L will be proportional to the sum of these two components. Subsequently, Detwiler et al. [47•] investigated the relationship between D_L and Pe for solute transport in a measured aperture field, demonstrating that D_L can be estimated reasonably well over a wide range of Pe by:

$$D_L/D_m = \alpha_m \mathrm{Pe} + \alpha_T \mathrm{Pe}^2 \quad (4)$$

where α_m is given by Gelhar's expression for macrodispersivity in a variable-aperture fracture, and $\alpha_T = 1/210$, the theoretical expression for Taylor dispersion between parallel plates. A unified theoretical analysis [Mallikamas and Rajaram, unpublished] further clarifies the foundations of Eq. (4), in particular the additivity of macrodispersion and Taylor dispersion. Experimentally measured values of D_L [47•] and the theoretical predictions based on Eq. (4) differ by approximately 25–40%, apparently due to the inability of the Reynolds equation (upon which the theory is based) to fully describe the three-dimensional velocity field within the fracture. Thus, more accurate estimates of D_L must be based on improved two-dimensional models of flow, or the three-dimensional Stokes equations.

Experimental studies of solute transport in fractures containing an entrapped phase have reported rapid solute movement in channels, holdup of solute in 'dead zones', and diffusive exchange between the two (e.g. [9•,10•]). Based on these observations, it is expected that the travel distance required for Fickian behavior would be substantially longer than under single-phase conditions. In addition, transport was observed to be very sensitive to differences in phase structure, even at similar values of phase saturation and relative permeability. These results were underscored in a recent study, where small errors in aperture field measurement were shown to have large influences on MIP phase-structure simulations, which in turn significantly influence the nature of calculated solute breakthrough curves [38••]. In a similar man-

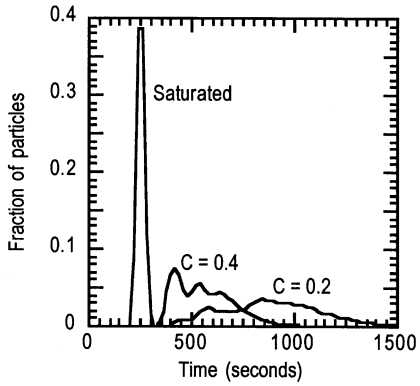

Fig. 4. Transport within fracture containing an entrapped phase: influence of curvature number, C. Particle tracking is used to simulate solute transport (from left to right) through the final satiated phase structures generated by the MIP model as shown in Fig. 1 and flow fields shown in Fig. 3. These solute concentration breakthrough curves (BTCs) measured at the downstream boundary of the fracture exhibit multiple peaks and are quite different for the two fields. A BTC in the absence of an entrapped phase is also shown.

ner, we illustrate the critical influence of phase structure by simulating transport through the flow fields shown in Fig. 3. Solute breakthrough curves (BTCs) for these fields, as well as for the single-phase case, are plotted in Fig. 4. For the single-phase case, the BTC is approximately Gaussian, indicating that, at the scale of this fracture, it may be appropriate to describe D_L using Eq. (4). However, for fields with entrapped phase, the BTCs become multi-modal and asymmetric, suggesting that a Fickian description of D_L is inappropriate. The dependence on phase structure and potential for non-Fickian behavior will complicate the development of an effective expression for D_L in fractures beyond that recently proposed for unsaturated porous media [48].

6. Mass transfer between phases

In addition to displacement processes (see Sections 2 and 3), inter-phase mass transfer may cause changes in phase structure. Examples of inter-phase mass transfer include: dissolution of an entrapped non-aqueous phase liquid (NAPL) into a flowing aqueous phase; dissolution and growth of gas bubbles; and dissolution or deposition of the fracture walls. Although dissolution of an immobile phase has been investigated extensively in laboratory-scale porous media (e.g. [49–51]), there are few studies in rough-walled fractures. There has also been recent interest in quantifying the dissolution dynamics of immobile NAPLs using pore-scale or other high-resolution models (e.g. [52–55]). Such models can incorporate details of the NAPL distribution at the pore-scale, and thus serve as a framework for predicting mass transfer rates based on pore structure parameters.

The only investigation of entrapped-phase dissolution in rough-walled fractures that we are aware of was reported by Glass and Nicholl [10•]. They showed that regions of high mass transfer did not correspond to locations of cluster shrinkage, nor was the path that an individual entrapped cluster shrinks given by SP or IP displacement models. However, subsequent MIP model application has shown good correspondence for cluster shrinkage path [11••]. Based on these results, and those presented in Sections 4 and 5, a depth-averaged computational approach has recently been developed for entrapped-phase dissolution [Detwiler, Rajaram and Glass, unpublished] that couples: fluid flow (modeled using the Reynolds equation in the flowing phase) and solute transport (modeled with the advection–diffusion equation); mass transfer from the entrapped phase into the flowing phase (assuming equilibrium at the interfaces); and consequent interface movement (modeled using the MIP algorithm). Simulations using this model are in excellent agreement with new experiments, reproducing both the temporal phase-structure shrinkage and total NAPL mass very well.

To illustrate the influence of the entrapped phase structure on the dissolution process, we apply this coupled model to the final satiated-phase structures presented in Figs. 1 and 3. Fracture-scale NAPL saturation (S_N) and relative permeability (k_{rf}) are plotted against time for the duration of the simulation in Fig. 5a. For the $C = 0.4$ field, S_N is initially almost half that of the $C = 0.2$ field, yet the time required for complete dissolution from the two fields is almost identical. An explanation for this behavior is evident in a plot of total mass-transfer rate (J) and k_{rf} against water saturation (S_f) (Fig. 5b). The relative permeabilities for the two fields exhibit similar dependence on S_f, but J displays markedly different behavior for the two fields. For the $C = 0.4$ field, J decreases steadily until all of the NAPL is dissolved, while for the $C = 0.2$ field, J first increases to almost twice its initial value before beginning to decrease. As evident in Fig. 6, a large part of this behavior results from the differential dissolution-channel growth within the entrapped phase, once again demonstrating the sensitivity of mass transfer to entrapped phase structure.

Highly fingered growth of dissolution channels within the entrapped phase has also been observed in the context of porous media [56]; a linear stability analysis has been used to quantify regimes of flow velocity and initial saturation under which a plane dissolution front becomes unstable [57]. These results for entrapped-phase dissolution are similar to those obtained in the context of reactive infiltration in

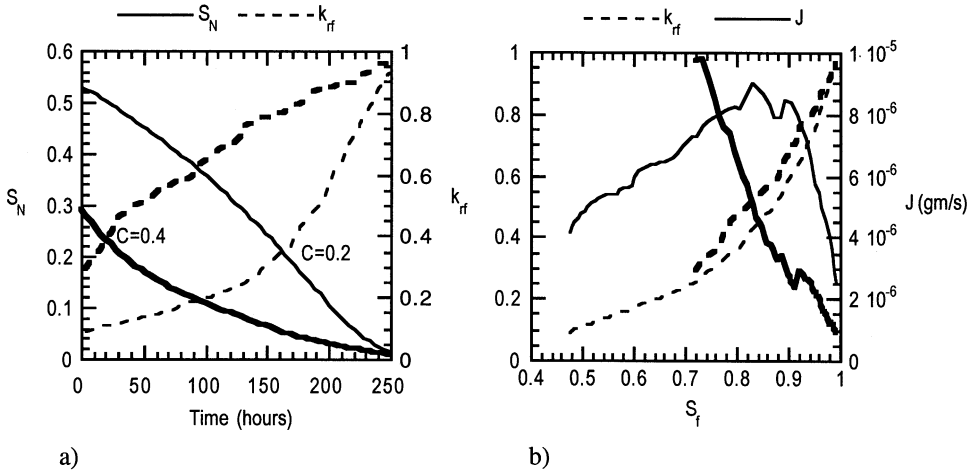

Fig. 5. Mass transfer between phases: dissolution of an entrapped phase and the influence of curvature number, C. Dissolution of the entrapped non-wetting phase from the $C = 0.2$ (thin lines) and $C = 0.4$ (thick lines) final satiated fields shown in Fig. 1 is simulated using the model developed by Detwiler, Rajaram, and Glass [unpublished]. The difference in the initial structure of the entrapped NAPL and the initial NAPL saturations (S_N) results in different behavior of the dissolution process with time (a). These differences can be understood by observing the differences in total mass-transfer rates (J) from the fracture as the NAPL dissolves (b). Though the NAPL dissolution process is very sensitive to the initial phase structure, the fracture scale relative permeability (k_{rf}) appears to be strongly dependent on the water saturation (S_f) in the fracture and less sensitive to differences in non-wetting phase structure. This result was also suggested by the experiments of Nicholl and Glass [9•].

soluble porous media (e.g. [58,59]). The related problem of dissolution of fracture walls by reactive fluids during single-phase flow has been recently investigated computationally [60••,61•,62], and experimentally [63]. Faster dissolution growth rates along preferential flow channels have been shown to lead to faster growth along these channels and a single, dominant dissolution-channel in time [60•,61]. Faster dissolution growth rates along preferential flow paths leads to faster channel growth along these paths. The fastest growing dissolution channel inhibits the growth of the other channels, and a single finger dominates. This behavior is consistent with Laplacian growth models, such as diffusion-limited aggregation (DLA) involving a linear flow equation, in which a single finger is predicted to dominate at large time (e.g. [64]).

7. Conclusions

Under conditions of two-phase, immiscible fluid flow, phase structure within the fracture ultimately controls the fluid pressure-saturation relations, permeability to each phase, solute dispersion within each phase, and inter-phase mass transfer. Research over the past 10 years has shown that phase structure will be a function of both the aperture field and the two-phase flow processes themselves. Capillary, gravitational, and viscous forces, in combination with boundary and initial conditions, have all been demonstrated to play roles in the determination of fracture phase structure. In the past 2 years, a suite of computational models has been developed and tested to simulate the development of phase structure, as well as flow and transport within each phase, and inter-phase mass transfer. Simulations in the absence of gravity or viscous forces show that entrapped phase structure varies systematically with the curvature number; flowing phase saturation increases and in-plane tortuosity decreases as the curvature number increases. These changes systematically influence the relative permeability at satiation and the transport of solute though the flowing phase, both of which fundamentally control inter-phase mass transfer. We believe that full parametric studies to consider the efficacy and parameterization of fracture-scale constitutive behavior for such situations are now in order.

Further extensions of this overall approach to include the influence of viscous and gravitational forces will facilitate further understanding of two-phase flow and transport processes under general conditions. However, advances on this front, even if more stimulating, will be slower. In the case of unstable displacements, experiments and modeling studies show highly channelized phase structures and flow paths, which in the case of gravity fingering, may pulsate and behave chaotically. In addition, the coupling between dissolution-precipitation or exsolution (e.g. degassing) reactions and permeability (or relative permeability) can lead to complicated flow-channeling phenomena and phase structure evolution. A general understanding of the morphology, connectivity, and temporal dynamics of all these channelized structures in rough-walled fractures is yet to be developed, and is a promising

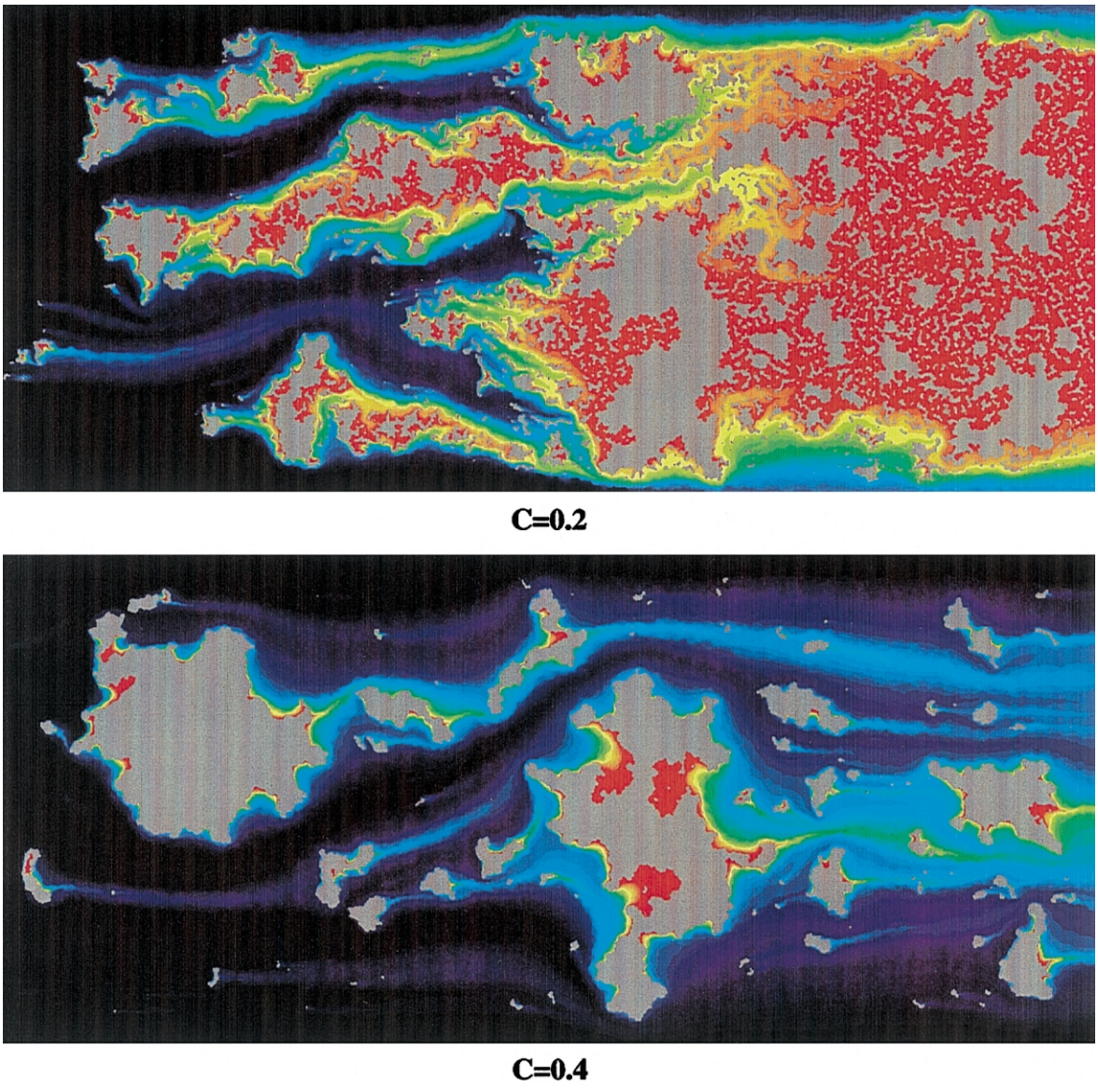

Fig. 6. Mass transfer between phases: dissolved phase concentration fields and the influence of curvature number, *C*. Dissolved non-wetting phase concentration fields as simulated using the model developed by Detwiler, Rajaram, and Glass [unpublished] are shown after 40% of the NAPL has been removed for the final satiated fields shown in Fig. 1. Gray denotes entrapped phase, while the color sequence black–blue–green–yellow–orange–red denotes non-wetting phase concentrations between 0 and the solubility limit within the flowing wetting phase. Dissolution channels develop down either side of the fracture, where entrapped phase could escape in the original phase displacement simulations. Internal dissolution channels develop very differently between the two fields due to the different initial satiated phase structures.

area for further research. This is a challenging problem, since several classical approaches to studying instabilities (e.g. linear stability analysis) do not explicitly recognize the role of medium heterogeneity, nor the mechanisms behind phase pulsation. Thus, it appears that a new paradigm must be developed to unify disparate observations in variable-aperture fractures and other disordered media.

Acknowledgements

Financial support for this review was provided by the U.S. Department of Energy's Basic Energy Sciences Geoscience Research Program under contract numbers DE-AC04-94AL85000 (Sandia National Laboratories), DE-FG03-96ER14590 (University of Colorado) and DE-FG03-01ER15122 (University of Idaho).

References and recommended reading

• of special interest
•• of outstanding interest

[1] •• Glass RJ, Nicholl MJ, Tidwell VC. Challenging models for flow in unsaturated, fractured rock through exploration of small-scale processes. Geophys Res Lett 1995;22(11): 1457–1460.

Paper synthesizes a large body of laboratory experiments focused on flow processes in single-fracture and fracture–matrix systems to surmise behavior of fluid flow in fracture networks and ensembles of matrix blocks. Large-scale channelized behavior is hypothesized that is inconsistent with current continuum scale models of flow through unsaturated fractured rock. This hypothesized behavior is supported by large-scale field evidence. An extended version including 43 figures was published by Sandia National Laboratories for the Yucca Mountain Project as SAND95-1824, 64 pp., 1996. Provides a basis upon which the current paper builds.

[2] National Research Council. Rock Fractures and Fluid Flow:
•• Contemporary Understanding and Applications, 1996.

Book reviews state of understanding across a large number of experts in the field. Fluid flow within fractures (mainly single phase with a small two-phase section) is presented, as well as many other topics in fractured media. Provides a very good summary of the entire fractured media field with respect to the subsurface.

[3] Stauffer D, Aharony A. Introduction to Percolation Theory. 2nd London: Taylor & Francis, 1992.

[4] Sahimi M. Flow phenomena in rocks: from continuum models
• to fractals, percolation, cellular automata, and simulated annealing. Rev Mod Phys 1993;65(4):1393–1534.

An excellent introduction to the topic of flow in porous media and provides a foundation upon which two-phase flow in fractures and fractured rock may be built. Indeed, the particular area of two-phase flow is called out as one where significant research had yet to be conducted.

[5] Glass RJ, Norton DL. Wetted region structure in horizontal unsaturated fractures: water entry through the surrounding porous matrix. Proceedings of the Third Annual International Conference on High-Level Radioactive Waste Management, 12–16 April 1992. Las Vegas, Nevada: American Nuclear Society, 1992:717–726.

[6] Reitsma S, Kueper BH. Laboratory measurement of capillary
• pressure–saturation relationships in a rock fracture. Water Resour Res 1994;30(4):865–878.

Study finds hysteresis in pressure–saturation relationships for a horizontal natural fracture and applies simplistic modeling to analyze the results; however, aperture field data could only be inferred. To us, this study demonstrates both that natural fractures will behave such as found previously in analog fractures [5], and are of limited usefulness to increase fundamental process understanding because measurements of aperture fields and phase structure are either precluded, or of insufficient accuracy.

[7] Wilkinson D, Willemsen JF. Invasion percolation: a new form of percolation theory. J Phys A: Math Gen 1983;16:3365–3376.

[8] Glass RJ. Modeling gravity-driven fingering in rough-walled fractures using modified percolation theory. Proceedings of the Fourth Annual International Conference on High-Level Radioactive Waste Management, 26–30 April 1993. Las Vegas, Nevada: American Nuclear Society, 1993:2042–2052.

[9] Nicholl MJ, Glass RJ. Wetting phase permeability in a par-
• tially saturated horizontal fracture. Proceedings of the Fifth Annual International Conference on High-Level Radioactive Waste Management, 22–26 May 1994. Las Vegas, Nevada: American Nuclear Society, 1994:2007–2019.

Presents measurements of fracture permeability at the satiated state in a transparent fracture. Entrapped phase structure is varied and quantitative transmitted-light imaging provides very detailed and accurate data on aperture and phase occupancy during flow. Provides foundation for evaluation of process-based effective media model. Widely varying phase structures created by different displacement histories displayed a relatively smooth functional relation between relative permeability and phase saturation; however, visual observation of dye pulses suggest that transport properties will be strongly dependent on phase structure.

[10] Glass RJ, Nicholl MJ. Quantitative visualization of entrapped
• phase dissolution within a horizontal flowing fracture. Geophys Res Lett 1995;22(11):1413–1416.

Uses quantitative light transmission imaging to measure aperture, phase, and entrapped phase shrinkage within a flowing fracture. Demonstrates that blob shrinkage avoids fragmentation, and that the location of phase shrinkage does not correspond with locations of high mass transfer. These results suggest that each blob of entrapped phase is in equilibrium, and that the path of shrinkage is controlled by full three-dimensional curvature that minimizes surface energy of the phase interface. During dissolution, satiated relative permeability (k_{rs}) is found to follow a power law in saturation.

[11] Glass RJ, Nicholl MJ, Yarrington L. A modified invasion
•• percolation model for low-capillary number immiscible displacements in horizontal rough-walled fractures: influence of local in-plane curvature. Water Resour Res 1998;34 (12):3215–3234.

MIP model including dynamic calculation of in-plane curvature at the displacement front is developed and compared to data for wetting invasion, non-wetting invasion and non-wetting phase dissolution. Model matches data extremely well, while SP and IP are deficient. A dimensionless curvature number is defined that weighs relative strength of in-plane and aperture-induced curvature. Results of a parametric study for both wetting and non-wetting invasion are presented and show significant influence of in-plane curvature on phase saturation and structure within a fracture.

[12] Homsy GM. Viscous fingering in porous media. Annu Rev Fluid Mech 1987;19:271–311.

[13] Nicholl MJ, Glass RJ, Nguyen HA. Gravity-driven fingering in unsaturated fractures. Proceedings of the Third Annual International Conference on High-Level Radioactive Waste Management, 12–16 April 1992. Las Vegas, Nevada: American Nuclear Society, 1992:321–331.

[14] Nicholl MJ, Glass RJ, Nguyen HA. Small-scale behavior of single gravity-driven fingers in an initially dry fracture. Proceedings of the Fourth Annual International Conference on High-Level Radioactive Waste Management, 26–30 April 1993. Las Vegas, Nevada: American Nuclear Society, 1993: 2023–2032.

[15] Nicholl MJ, Glass RJ, Nguyen HA. Wetting front instability in an initially wet unsaturated fracture. Proceedings of the Fourth Annual International Conference on High-Level Radioactive Waste Management, 26–30 April 1993. Las Vegas, Nevada: American Nuclear Society, 1993:2061–2070.

[16] Nicholl MJ, Glass RJ, Wheatcraft SW. Gravity-driven infil-
•• tration flow instability in non-horizontal unsaturated fractures. Water Resour Res 1994;30(9):2533–2546.

Demonstrated gravity-driven fingering in rough-walled fractures as a separate mechanism from capillary heterogeneity. Showed instability from three different boundary conditions in an analog fracture. Finger location and width were dependent on configuration of the interface at the onset of instability. Transmitted light imaging revealed drainage behind the finger tip, and provided data relating tip length to finger velocity. A conceptual model based on interplay of capillary, gravity, and viscous forces fit the data very well for tip/blob dynamics.

[17] Glass RJ, Nicholl MJ. Physics of gravity-driven fingering of immiscible fluids within porous media: an overview of current understanding and selected complicating factors. Geoderma 1996;70(2–4):133–163.

[18] Fourar M, Bories S, Lenormand R, Persoff P. Two-phase flow in smooth and rough fractures: measurement and correlation by porous-medium and pipe-flow models. Water Resour Res 1993;29(11):3699–3708.

[19] • Persoff P, Pruess K. Two-phase flow visualization and relative permeability measurement in rough-walled fractures. Water Resour Res 1995;31(5):1175–1186.

Measurements of relative permeability under conditions of concurrent flow are presented. Significant phase interference led to flow pulsation. Concurrent flow, such as explored here, is important in geothermal applications where flows are highly forced.

[20] • Su GW, Geller JT, Pruess K, Wen F. Experimental studies of water seepage and intermittent flow in unsaturated, rough-walled fractures. Water Resour Res 1999;35(4):1019–1037.

Study follows up on the work of Nicholl et al. [13–16••] where flow pulsation was demonstrated. Both replicas of natural fractures and fabricated systems are used to elucidate mechanism. However, a more recent study [65] suggests that epoxy replicas and plastics as used in this work may have different behavior than other surfaces more representative of rock or glass.

[21] Longino BL, Kueper BH. Non-wetting phase retention and mobilization in rock fractures. Water Resour Res 1999;35(7):2085–2093.

[22] • Zhong, L, Mayer A, Glass RJ. Visualization of surfactant-enhanced NAPL mobilization and solubilization in a two-dimensional micro-model. Water Resour Res 2001; 37(3):523–537.

Considers experimentally the mobilization and subsequent dissolution of an entrapped NAPL by a series of floods where flow rate or chemistry (surfactant) is varied. An analog rough-walled fracture is used where the aperture field and entrapped phase structure/saturation was measured with high accuracy. Finds final saturation after mobilization to be different for the same capillary/viscous ratio, depending on whether a surfactant solution or pure water was used. Micro-scale processes are responsible for the difference. When surfactant first encounters the upstream edge of NAPL blobs, reduced capillary forces there drive the NAPL upstream to create a high saturation 'bank' perpendicular to the direction of flow. However, for viscous mobilization, NAPL moves as rivulets oriented in the direction of flow and avoids much of the field to leave a much lower final NAPL saturation.

[23] Amundsen H, Wagner G, Oxaal U, Meakin P, Feder J, Jossang T. Slow two-phase flow in artificial fractures: experiments and simulations. Water Resour Res 1999;35 (9):2619–2626.

[24] • Xu B, Yortsos YC, Salin D. Invasion percolation with viscous forces. Phys Rev E 1998;57(1):739–751.

While this study considers porous media, it is important as it includes viscous forces into an MIP model. Results are compared to some stable displacement studies with excellent results. An approach along these lines that includes gravity, as well as an additional second-order viscous effect, has subsequently been shown to model experiments in heterogeneous porous media well [26].

[25] Ewing RP, Berkowitz B. A generalized growth model for simulating initial migration of dense non-aqueous phase liquids. Water Resour Res 1998;34(4):611–622.

[26] Glass RJ, Conrad SH, Yarrington L. Gravity-destabilized non-wetting phase invasion in macroheterogeneous porous media: near pore-scale macro modified invasion percolation model. Water Resour Res 2001;37(5):1197–1207.

[27] Szep J, Cserti J, Kertesz J. Monte Carlo approach to dendritic growth. J Phys A: Math 1985;18:L413–L418.

[28] • Zimmerman RW, Bodvarsson GS. Hydraulic conductivity of rock fractures. Transp Porous Media 1996;23:1–30.

Excellent starting point for exploring single-phase flow in a discrete fracture. Clear discussions regarding simplification of the Navier–Stokes equations to the Reynolds equation, effective media approaches, and effects of contact area.

[29] Ge S. A governing equation for fluid flow in rough fractures. Water Resour Res 1997;33(1):53–61.

[30] Koplik J, Ippolito I, Hulin JP. Tracer dispersion in rough channels — a 2-dimensional numerical study. Phys Fluids A 1993;5(6):1333–1343.

[31] • Brown SR, Stockman HW, Reeves SJ. Applicability of the Reynolds equation for modeling fluid flow between rough surfaces. Geophys Res Lett 1995;22:2537–2540.

Comparison of Reynolds equation to lattice-gas simulations (LGA) for 2-D flow between sinusoidal surfaces helps illuminate inadequacies of the Reynolds equation. LGA shows non-parabolic velocity profile and counter-current flow under some conditions.

[32] Gutfraind R, Ippolito I, Hansen A. Study of tracer dispersion in self-affine fractures using lattice-gas automata. Phys Fluids 1995;7(8):1938–1948.

[33] Waite ME, Ge S, Spetzler H, Bahr DB. The effect of surface geometry on fracture permeability: a case study using a sinusoidal fracture. Geophys Res Lett 1998;25(6):813–816.

[34] Dijk P, Berkowitz B, Bendel P. Investigation of flow in water-saturated rock fractures using nuclear magnetic resonance imaging (NMRI). Water Resour Res 1999;35 (2):347–360.

[35] • Mourzenko VV, Thovert JF, Adler PM. Permeability of a single fracture— validity of the Reynolds equation. J Phys II 1995;5(3):465–482.

Flow fields computed using the Stokes and Reynolds equations are compared on computer-generated fracture geometries. The Reynolds equation is found to overestimate the overall transmissivity by as much as a factor of two, when compared to the Stokes equation. However, it appears that the aperture-field statistics for most of the fractures they consider are in a range where previous studies (e.g. [28•]) suggest that the Reynolds equation will not be very accurate.

[36] Yeo IW, De Freitas MH, Zimmerman RW. Effect of shear displacement on the aperture and permeability of a rock fracture. Int J Rock Mech Miner Sci 1998;35(8):1051–1070.

[37] Renshaw CE, Dadakis JS, Brown SR. Measuring fracture aperture: a comparison of methods. Geophys Res Lett 2000;27(2):289–292.

[38] •• Detwiler RL, Pringle SE, Glass RJ. Measurement of fracture aperture fields using transmitted light: an evaluation of measurement errors and their influence on simulations of flow and transport through a single fracture. Water Resour Res 1999;35(9):2605–2617.

Description of a light transmission system for measuring fracture aperture in transparent models of fractures at high spatial resolution. Includes a detailed investigation of the factors leading to measurement errors and presents a measurement protocol to minimize and quantify remaining errors. They also demonstrate the sensitivity of simulations for single- and two-phase flow and transport to errors in aperture field measurements.

[39] • Nicholl MJ, Rajaram H, Glass RJ, Detwiler R. Saturated flow in a single fracture: evaluation of the Reynolds equation in measured aperture fields. Water Resour Res 1999;35 (11):3361–3373.

The Reynolds equation is tested against experiments using highly accurate aperture data from specifically designed analog fractures. Over-prediction of measured flow by 22–47% well exceeds $\sim 1\%$ experimental error. Simulations converge at a data resolution of $\sim 1/5$ of the aperture correlation scale; outcomes are shown to be sensitive to numerical formulation and method of data collection; i.e. point vs. averaged.

[40] Gelhar LW. Stochastic Subsurface Hydrology. Prentice-Hall, 1993.

[41] Pruess K, Tsang YW. On two-phase relative permeability and capillary pressure of rough-walled rock fractures. Water Resour Res 1990;26(9):1915–1926.

[42] Kwicklis EM, Healy RW. Numerical investigation of steady

liquid water flow in a variably saturated fracture network. Water Resour Res 1993;29(12):4091–4102.

[43] • Nicholl MJ, Rajaram H, Glass RJ. Factors controlling satiated relative permeability in a partially saturated horizontal fracture. Geophys Res Lett 2000;27(3):393–396.

Developed new conceptual model for satiated relative permeability from effective medium theory and previous experimental observations. In-plane tortuosity is shown to be the dominant factor in controlling flow, followed by saturation of the flowing phase.

[44] Dronfield DG, Silliman SE. Velocity dependence of dispersion for transport through a single fracture of variable roughness. Water Resour Res 1993;29(10):3477–3483.

[45] • Ippolito I, Daccord G, Hinch EJ, Hulin JP. Echo tracer dispersion in model fractures with a rectangular geometry. J. Contam Hydrol 1994;16(1):87–108.

Uses solute transport experiments in a rough-walled fracture to demonstrate distinct macrodispersion and Taylor dispersion regimes and empirically fit their data with an expression similar to Eq. (4). They suggest that the macrodispersion contribution would be related to fracture roughness.

[46] • Roux S, Plouraboue F, Hulin JP. Tracer dispersion in rough open cracks. Transp Porous Media 1998;32(1):97–116.

Presents a scaling analysis of solute dispersion in rough-walled fractures to support the empirical evidence of [45•] that D_L can be represented as a sum of macrodispersion and Taylor dispersion components. Suggested that the macrodispersion term is proportional to the variance and correlation length of the aperture field.

[47] • Detwiler RL, Rajaram H, Glass RJ. Solute transport in variable-aperture fractures: an investigation of the relative importance of Taylor dispersion and macrodispersion. Water Resour Res 2000;36(7):1611–1625.

Experimentally demonstrates the transition between the macrodispersion and Taylor dispersion controlled regimes for longitudinal dispersion in a variable-aperture fracture. A theoretical expression (Eq. (4) of this paper) for the dispersion coefficient applicable across both regimes is proposed, which illustrates that aperture variability statistics control the Peclet number value where the transition occurs. Three-dimensional solute transport simulations consistently reproduced both the Taylor dispersion and macrodispersion regimes, but underestimated dispersivity values observed in the experiments by 25–40%. Discrepancies between theory and experiments are hypothesized to be due to the inability of the Reynolds equation (upon which the theory was based) to fully describe the three-dimensional velocity field in the fracture.

[48] Padilla, IY, Yeh T-CJ, Conklin MH. The effect of water content on solute transport in unsaturated porous media' Water Resour Res 1999;35(11):3303–3314.

[49] Powers SE, Abriola LM, Weber Jr WJ. An experimental investigation of non-aqueous phase liquid dissolution in saturated subsurface systems: steady-state mass transfer rates. Water Resour Res 1992;27(4):463–477.

[50] Geller JT, Hunt JR. Mass transfer from non-aqueous phase organic liquids in water-saturated porous media. Water Resour Res 1993;29(4):833–845.

[51] Imhoff PT, Jaffe PR, Pinder GF. An experimental study of complete dissolution of a non-aqueous phase liquid in saturated porous media. Water Resour Res 1994;30(2):307–320.

[52] Kennedy CA, Lennox WC. A pore-scale investigation of mass transport from dissolving DNAPL droplets. J Contam Hydrol 1997;24:221–246.

[53] Jia C, Shing K, Yortsos YC. Visualization and simulation of non-aqueous phase liquid solubilization in pore networks. J Contam Hydrol 1999;35:363–387.

[54] Dillard LA, Blunt MJ. Development of a pore network simulation model to study non-aqueous phase liquid dissolution. Water Resour Res 2000;36:439–454.

[55] Held RJ, Celia MA. Pore-scale modeling extension of constitutive relationships in the range of residual saturations. Water Resour Res 2001;37(1):165–170.

[56] Imhoff PT, Miller CT. Dissolution fingering during the solubilization of non-aqueous phase liquids in saturated porous media, 1. Model predictions. Water Resour Res 1996; 32(7):1919–1928.

[57] Imhoff PT, Thyrum GP, Miller CT. Dissolution fingering during the solubilization of non-aqueous phase liquids in saturated porous media, 2. Experimental observations. Water Resour Res 1996;32(7):1929–1942.

[58] Chadam J, Hoff D, Merino E, Ortoleva P, Sen A. Reactive infiltration instabilities. J Appl Math 1986;36:207–221.

[59] Sherwood JD. Stability of a plane reaction front in a porous medium. Chem Eng Sci 1987;42(7):1823–1829.

[60] • Bekri S, Thovert J-F, Adler PM. Dissolution and deposition in fractures. Eng Geol 1997;48(3-4):283–308.

Detailed computational study coupling the Stokes equation for flow, solute transport equation and time variation of apertures due to dissolution or deposition. Dissolution, deposition and dissolution-deposition cycles are investigated. Non-repeating dissolution and deposition patterns are observed during the dissolution-deposition cycles. Control of dissolution patterns by Damkohler and Peclet numbers is also demonstrated.

[61] • Hanna RB, Rajaram H. Influence of aperture variability on the dissolutional growth of fissures in karst formations. Water Resour Res 1998;34(11):2843–2853.

Computational study demonstrating the influence of aperture variability statistics on fracture wall dissolution channels. The dissolution channels are shown to be narrower and more tortuous with increased aperture variance. Increased aperture variance is also shown to increase the rate of growth of the overall fracture transmissivity, which has important implications for geological processes such as karstification.

[62] Rajaram H, Cheung W, Hanna RB. Potential influence of aperture variability on dissolutional enlargement of fissures. In: Palmer AN, Palmer MV, Sasowsky ID, editors. Karst Modeling, Proceedings of the Symposium held 24–27 February 1999, Charlottesville, Virginia. Karst Waters Institute, 1999. Special Publication No 5.

[63] Durham WB, Bourcier WL, Burton EA. Direct observation of reactive flow in a single fracture. Water Resour Res 2000;37 (1):1–13.

[64] Meakin P. Fractal aggregates in geophysics. Rev Geophys 1991;29:317–354.

[65] Wan J, Tokunaga TK, O'Neil J, Thomas RO. Glass casts of rock fracture surfaces: a new tool for studying flow and transport. Water Resour Res 2000;36(1):355–360.